

Effect of Injecting Inert Particles on Coking Prohibition and Particle Velocity Uniformization in Downer Reactors

ZHANG Jiyu(张济宇)^{a,*}, ZHU Yuan(祝媛)^a, Tian Yajun(田亚峻)^b and XIE Kechang(谢克昌)^b

^a Institute of Chemical Engineering and Technology, Fuzhou University, Fuzhou 350002, China

^b Education Ministry Key Lab of Coal Science and Technology, Taiyuan University of Technology, Taiyuan 030024, China

Abstract The coking observation and particle flow behaviour in both thermal plasma and cold plexiglas downers were investigated in a binary particle system formed by injecting coarse inert particles (carrying coke away and scouring wall) and fine coal powders into the downer reactor. The results demonstrate that this scheme is a rational selection to prevent coking on downer walls and improve particle velocity distribution along the radial direction. When injected coarse particles mixed with fine powders in downers, the fluctuation of local particle velocity in the radial direction becomes smaller and two peaks in the radial distribution of local particle velocity occur due to the improved dispersing character and flow structure, which are beneficial to the thermo-plasma coal cracking reaction and coking prevention.

Keywords thermal plasma, coking, downer, particle velocity, binary mixture

1 INTRODUCTION

The thermal plasma technology and the downer reactor has been used for coal pyrolysis to produce acetylene for about 50 years[1], but serious coking appearing in the downer reactors is the deteriorating factor to the stable and continuous operation of this process[2–6]. As pointed by Zhu *et al.*[7] that when injecting appropriate amount of inert particles and coal into downer, the problem of coking could be prohibited or alleviated since the inert particles can carry the coking precursor away and also scour the downer wall to draw the coking matter off. Therefore, a binary particle mixture system composed of inert and reactant particles is present in downer and causes some changes in flow behavior, which becomes a new problem to be clarified. In order to resolve the coking problem in thermal plasma coal pyrolysis process (TPCPP), it is necessary to perform the special and systematic study on the coking phenomenon, solid mixing and flow characteristics in downer reactors with injected binary particle mixture.

2 COKING PROBLEM IN HOT MODE EXPERIMENT

2.1 Coking mechanism

In the thermal arc plasma downer reactor, the arc plasma jet, formed by hydrogen or other gas passing through an arc, not only exhibits very high temperature, but also contains a large number of activated hydrogen ions and atoms. Thus, under high temperature, these activated species will break the chemical bonds of large molecular structure in the coal and result in the coal cracking and further conversion to many new species, such as CH-groups (C_nH_m), free carbons (nC), residual chars, and primary volatiles, all being called coking precursors. These primary volatiles also could be further cracked, polymerized, compounded to the

final products, such as gas, residual chars and coking. In view of the chemistry the produced coking precursor is the original reason for coking[6,8]. Furthermore, due to the action of thermo-phoresis force and centrifugal force from the arc plasma jet in the high temperature zone of the thermal arc plasma downer, one of the coking precursors, nC , will come into collision with downer walls and together with the fusible ash will stick on downer walls. In the middle temperature zone the coking precursor C_nH_m , appearing in small liquid drops and composed of polymers or compounds with high molecular weight, also have the possibility of contacting and sticking to the wall, then being carbonized into coking. In the low temperature zone the coking precursor, *i.e.* residual chars, will deposit on walls and form coking. All of the above are the practical reasons[6] for coking from the physical point of view.

2.2 Experimental apparatus and scheme

The hot mode of TPCPP was composed of the arc plasma generator (cathode 1, insulation 2, anode 3, arc 4), feeding distributor (injector 5), downer reactor 6, spray quencher 7 and separator 8 as shown in Fig.1. The reactants [liquefied petroleum gas (LPG) or coal powders] together with the carrying argon gas were injected by an injector (5) into the top of the downer reactor (6). The pyrolysis of reactants was carried out in a 350mm long downer reactor (6) with 20mm diameter. In this downer the hard carbon (or graphite) tube used as lining was put in inner wall and the water jacket was set up in outer wall to prevent the inner wall breakage by the high temperature plasma jet. The product gas before entering the separator (8), connected with the bottom of the downer reactor (6), was quenched by the cool water spray to reduce further decomposition of acetylene and then it flowed out

Received 2005-11-21, accepted 2006-03-26.

* To whom correspondence should be addressed. E-mail: jy Zhang@fzu.edu.cn

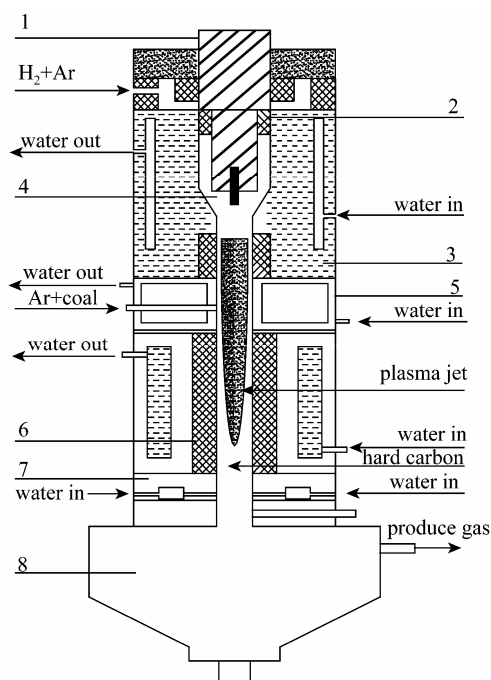


Figure 1 Scheme of the arc plasma downer for hot model
1—cathode; 2—insulation; 3—anode; 4—arc; 5—injector;
6—downer reactor; 7—spray quencher; 8—separator

from the top of the separator (8). A detailed experimental procedures can refer to Tian[6].

2.3 Prevention of coking

As mentioned above the coking mechanism, the original coking mechanism from the coking precursor is unavoidable, but the practical coking due to physical action is avoidable. Therefore, based on the concept of inert particles as no-coke carriers and wall scourer, the problem of coking in TPCPP could be alleviated and prohibited ultimately by injecting an appropriate amount of inert particles and together with coal powders into downers, which had already been pointed out by Zhu *et al.*[7].

Since the coking deposition on downer walls for the LPG cracking is more serious than that of the coal powder cracking[6], the LPG cracking can be used to evaluate the coking prevention by injecting the metallurgical coke (MC) as the inert coking carrier and wall scourer. The coking depositions on the inner walls of the downer reactor can be collected by scraping the downer walls after each experiment. Therefore, the coking rate (R_{ck} , $g \cdot s^{-1}$), defined as the coking increment per unit time, can be calculated by the total coking depositions divided by the total reaction time and it is used to indicate the strength of wall coking. The comparison of R_{ck} for LPG cracking under the easily coking condition, *i.e.* the LPG flow rate being $1.36m^3 \cdot h^{-1}$ is summarized in Table 1. It is clear that the highest $R_{ck}=0.15g \cdot s^{-1}$ occurs in the LPG cracking process without adding MC in the thermo-plasma downer, and the serious and thick annual coking around the whole downer walls is sketched in the last row of Table 1. The R_{ck} decreased distinctly with in-

jected MC particles. When the size of MC further increased to above $0.246mm$, R_{ck} reduced quickly to below $0.0314g \cdot s^{-1}$, even almost eliminated when larger MC particles were injected.

When feeding the coarse MC ($\bar{d}_p=0.59$) into the thermal plasma downer reactor of 20mm I.D. and 350mm long during the LPG cracking process, no coking and blocking appear on the downer walls even though the cracking time is about twice that of the experimental run without any MC in the LPG cracking, seeing the experimental number 4 in Table 1. This means that the coarse MC is a better selection as the inert coking carrier and wall scourer. During the LPG cracking process in the thermo-plasma cracking downer, the coking precursor from LPG cracking will deposit on the down-flowing MCs since these injected MC particles can firstly touch and adhere to the coking precursor before it diffusing toward the wall and forming cokes on the downer walls. Therefore, the stable and continuous operation will be achieved in the LPG thermo-plasma cracking.

When a binary coal mixture, composed of fine and coarse coal particles, are used in the thermo-plasma downer for the process of acetylene production from coal cracking, the fine coals are easily cracked to produce the acetylene gas, only a small part of coarse coals may be cracked and the rest will carry the coking precursor generated from pyrolysis of fine coals and scour the downer wall to carry the coking matter away. Therefore, an appropriate size of coarse coal and certain ratio of coarse to fine coal are necessary to prevent coking on walls and to provide higher acetylene yield. Their experimental results about coking status in thermo-plasma downer reactor are listed in Table 2[9]. Obviously, when the mass ratio of coarse coal ($d_p=0.246-0.351mm$) to fine coal ($d_p<0.119mm$), *i.e.* D/A, is 30/70, no coking on the wall occurs in the downer tube during experiment. This demonstrates again that the coarse coal particles, with an appropriate size above $0.246mm$ as mentioned in the LPG thermo-plasma cracking, can play the role of inert coking carrier and scour the downer tube in the process of acetylene production from coal cracking.

3 FLOW BEHAVIOR IN THE COLD MODE

3.1 Experimental apparatus and scheme

From the above hot experimental demonstration in a thermal plasma downer, a corresponding cold model with a similar scale, composed of a semicircular downer of 30mm I.D. and 2m tall, was established in our lab as shown in Fig.2, which consisted mainly of a feeding part (feeder 1, rotameter 8), gas-solids downer compartments (gas-solids distributor 2, downer 3, fast separator 7) and a PV-4A particle velocity measurement system (fiber-optic probe 4, PV-4A velocity instrument 5, sample tube 6).

Two kinds of materials [some coarse particles-glass beads simulating the inert particles and the bulk fluidized-bed catalytic cracking (FCC) powders as the reactant] are injected individually from respective feeders by the T-type pneumatic valve simultaneously

Table 1 The comparison of coking rate (R_{ck}) for LPG cracking

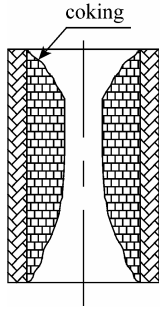
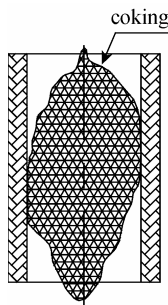
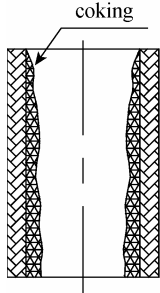
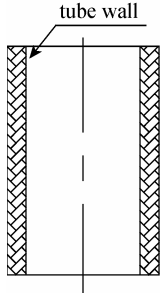
Exp. number	Size of MC, mm	Feed rate of MC, $g \cdot s^{-1}$	Cracking time, s	$R_{ck}, g \cdot s^{-1}$	Coking phenomena	Sketch of coking on the wall
1	No MC addition	0	220	0.15	Serious and thick annual coking around the whole walls of downer tube; the inner diameter of the whole downer was reduced from original size 20mm to 5mm.	
2	0.175—0.246 (80—60 mesh) ($\bar{d}_p=0.21$)	2.5—3.3	197	0.0731—0.0814	Lighter and thin annual coking around the whole walls of downer tube; the lump coke with a jujube pit shape formed at the center of lower part in downer.	
3	0.246—0.351 (60—40 mesh) ($\bar{d}_p=0.30$)	3.64—4	210	0.0241—0.0314	Some linear cokes like vitreous body formed on the upper wall of downer tube; the inner diameter of the whole downer was little less than that of original size.	
4	0.351—0.833 (40—20 mesh) ($\bar{d}_p=0.59$)	2.61—4.37	410	0.0043—0.0136	A few point cokes appear as vitreous body formed on the upper wall of downer tube; the inner diameter of the whole downer still was original size.	

Table 2 Effect of coarse/fine ratio of coal on coking in thermo-plasma downer[9]

Coal	B/A: 30/70	C/A: 30/70	D/A: 30/70
Shenfu	thin coke zone	no coke	no coke
Pingshuo	coking	thin coke zone	no coke

Note: A: fine (>140 mesh, *i.e.* <0.119 mm); B: coarse (80—100 mesh, *i.e.* 0.147—0.175mm); C: coarse (60—80 mesh, *i.e.* 0.175—0.246mm); D: coarse (40—60 mesh, *i.e.* 0.246—0.351mm).

from different entrances into the downer, then fall down to the separator and returned to the top feeders by another pneumatic transport line, thus completing the solids

circulation. The material properties are given in Table 3.

During the cold model experiment the axial and radial distributions of local particle velocity at eight different radial positions ($r \cdot R^{-1}=0, 0.133, 0.267, 0.400, 0.533, 0.733, 0.866, 0.975$) on six various axial levels ($Z=110, 200, 290, 335, 425, 515$ mm) along the downer-column from top to bottom were measured by using a PVA-4 fiber-optic particle velocity probe and the effects of operation conditions (superficial gas velocity $u_g=0.785\text{--}3.139\text{m} \cdot \text{s}^{-1}$ and solid flow rate $G_s=7.5\text{--}14.9\text{kg} \cdot \text{m}^{-2} \cdot \text{s}^{-1}$) and binary materials (FCC and glass beads) on the local particle velocity (v_p) were examined in this investigation.

Table 3 Particle properties

	Material	d_p , mm	\bar{d}_p , mm	ρ_s , $\text{kg}\cdot\text{m}^{-3}$
fine	FCC	0.04—0.1	0.071	1500
coarse	glass bead 1	0.351—0.833 (40—20 mesh)	0.592	2658
	glass bead 2	0.246—0.351 (60—40 mesh)	0.345	2658

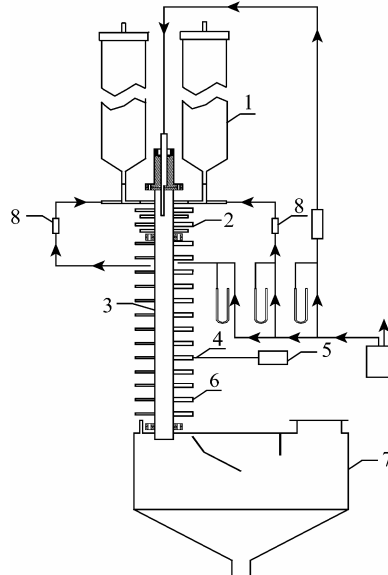


Figure 2 Experimental apparatus for cold mode

1—feeder; 2—gas-solids distributor; 3—downer;
4—fiber-optic probe; 5—PV-4A velocity instrument;
6—sample tube; 7—fast separator; 8—gas rotameter

3.2 Axial variation of local particle velocity

Under $u_g=1.1\text{m}\cdot\text{s}^{-1}$ and $1.97\text{m}\cdot\text{s}^{-1}$ and $G_p=9.4\text{kg}\cdot\text{m}^{-2}\cdot\text{s}^{-1}$, the radial distribution of v_p for fine FCC powders at different axial positions, *i.e.* at $Z=110$, 200, 290, 335, 425, 515mm, are shown in Figs.3(a) and 3(b), respectively. It is well known that particles agglomerate easily near downer walls, due to low gas velocity arisen from wall friction and turbulence be-

tween gas and solids. Therefore, a lower drag force between gas and solids will take place at that position, which causes uneven radial distribution of v_p . At the lower gas velocity $u_g=1.1\text{m}\cdot\text{s}^{-1}$ and $Z=335\text{mm}$, v_p is small at the center and gradually increases from center to the wall, and the maximum v_p occurs at $r\cdot R^{-1}=0.8$ near the wall, then it decreases with further approach to the wall, which seems to be the typical radial distribution of v_p reported by Zhang *et al.*[10,11]. However, at the higher gas velocity $u_g=1.97\text{m}\cdot\text{s}^{-1}$ and $Z=200\text{mm}$, the radial profile of v_p evolves to the typical radial distribution of v_p .

For coarse glass beads 1 and 2, the corresponding radial profiles of v_p are smoother than that for fine FCC particles and v_p increases gradually along the axial distance especially when $Z\geq 335\text{mm}$ as depicted in Figs.3(c) and 3(d). Since the diameter and density of glass beads are respectively 8.3 and 1.8 times that of FCC, the glass beads undergo quick gravitational acceleration and reach easily the value of u_g and beyond its first accelerated section, making v_p display a more uniform radial distribution.

As mentioned above, for either FCC or glass beads in the cold model, v_p at $Z=335\text{mm}$ exhibits sufficient development, therefore $Z=335\text{mm}$ can be chosen as an appropriate fixed axial position to determine the radial distribution of v_p for the comparison between both single and binary particle system in this study[12].

3.3 Radial distribution of dimensionless local particle velocity

With the same gas-solids distributor and feeding

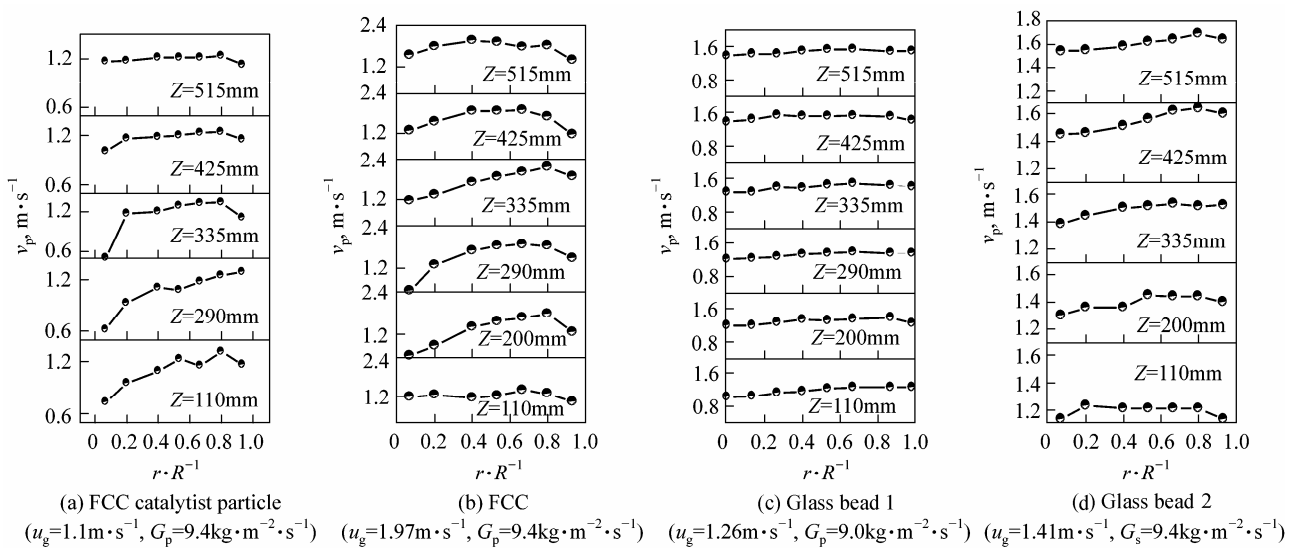
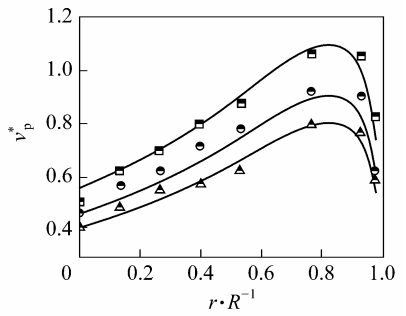
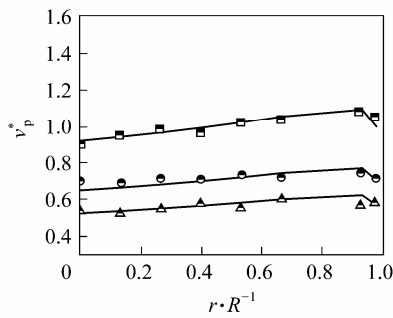


Figure 3 Radial profiles of local particle velocity at various axial positions

system, v_p measured at $Z=335\text{mm}$ in different radial position (r/R) changes with some factors, such as u_g , G_p , and particle properties (d_p , ρ_p). It is clear that in the downer of different size the variation of radial distribution of v_p differs, and no common correlation to estimate this variation is reported in the literature. In order to compare these diversities of radial profile of v_p , a dimensionless local particle velocity (v_p^*), i.e. the ratio of v_p to u_g , is introduced here to represent the profile variations with the ratio of r to R and different particles, which are shown in Fig.4.



(a) FCC
 u_g/G_p : ■ 1.97/14.1; ● 2.36/13.3; ▲ 2.72/13.2



(b) Glass beads 1
 u_g/G_p : ■ 1.26/9.1; ● 1.97/9.2; ▲ 2.52/9.0

Figure 4 Radial profiles of dimensionless local particle velocity at $Z=335\text{mm}$, $h_1=35\text{mm}$

For fine FCC particle belong to Geldarts' A group, the aeration and agglomerating properties between particles make v_p^* near wall fall rapidly and a large velocity gradient occur [in Fig.4(a)]. For coarse glass beads with un-agglomerating properties, the weak effect of wall friction results in a smooth radial profile of v_p^* [Fig.4(b)]. Therefore, the solid type, solid dispersion in gas flow and particle motion will dominantly affect the radial profile of v_p^* . Based on collected 320 data at the second acceleration and stable motion sections from the literature[10,11,13,14] and this study as listed in Table 4, a dimensionless empirical correlation of v_p^* for FCC and glass beads is given respectively by non-linear regressing on experimental data as below.

For FCC:

$$v_p^* = 1.63 \left(1 - \frac{r}{R}\right)^{\frac{1}{7}} \exp \left[-9 \left(1 - \frac{r}{R}\right)^{(H/D_t)^{0.5}} + 15 \right] \left(\frac{G_p}{u_g \rho_p} \right)^{0.8} \quad (1)$$

For glass beads:

$$v_p^* = 1.42 \left(1 - \frac{r}{R}\right)^{\frac{1}{7}} \exp \left[-17 \left(1 - \frac{r}{R}\right)^{(H/D_t)^{0.71}} + 23 \right] \left(\frac{G_p}{u_g \rho_p} \right)^{0.8} \quad (2)$$

where $[G_p/(u_g \rho_p)]$ is the dimensionless mean section particle velocity while assuming particles uniformly distributed in the whole downer section, and H/D_t is the ratio of height to downer diameter. The valid range of above correlations are $u_g=1.8-10.1\text{m}\cdot\text{s}^{-1}$ and $G_p=7.5-101\text{kg}\cdot\text{m}^{-2}\cdot\text{s}^{-1}$ and the correlation coefficient is 0.96. The deviation between calculated and experimental values are within $\pm 18\%$ as shown in Fig.5. The typical comparison between simulated solid curves using Eq.(1) for FCC and Eq.(2) for glass beads and measured v_p^* data is shown respectively in Figs.4(a) and 4(b), indicating a good agreement. The similarity of above two correlations may imply that a universal correlation could be proposed for different materials including the FCC, glass beads and other particles, which has been reported in Zhu's thesis[15].

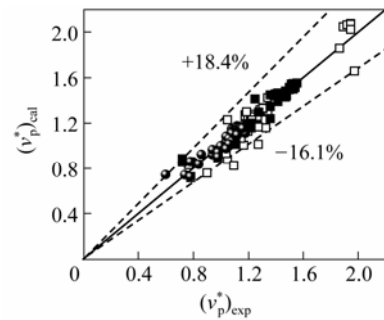


Figure 5 Comparison between the calculated v_p^* and the experimental ones

△ Yang *et al.*[11]; ■ Zhang *et al.*[12]; ◇ FCC, this work; □ Zhang *et al.*[8]; ◁ glass bead, this work; ● Lehner *et al.*[14]

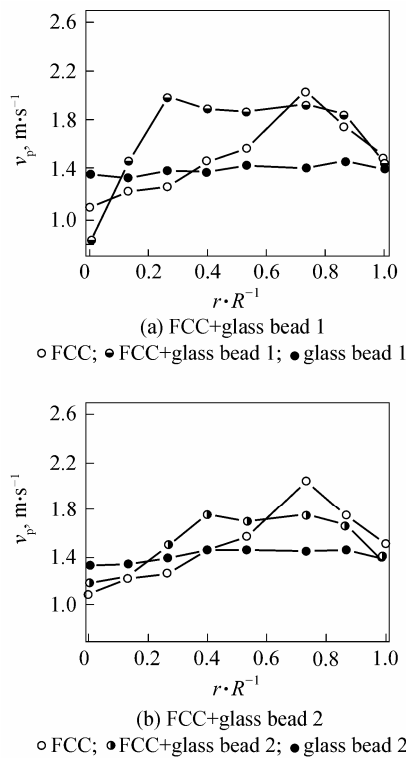
3.4 Radial distribution of local particle velocity of binary mixture

Finally, the radial distributions of the binary mixture particle velocity, created by simultaneously injecting coarse-glass beads at the upper entrance and fine-FCC catalysts at the lower entrance into the downer, were examined under different conditions of the composition ratio of glass beads to mixtures (M^*), u_g , and the relative entrance positions for glass beads and FCC. At $M^*=0.15$ and $u_g=1.97\text{m}\cdot\text{s}^{-1}$ the experimental results indicate that a more uniform profile of v_p and radial distribution with two peaks occurring either for FCC and glass beads 1 in Fig.6(a) or glass beads 2 in Fig.6(b). For the case of injecting FCC only, single peak of v_p profile is at $r\cdot R^{-1}=0.733$, but for the FCC and glass beads mixture system except a peak at $r\cdot R^{-1}=0.733$, a second peak also occurs around $r\cdot R^{-1}=0.4$, which causes the radial distribution of v_p becomes smooth and flat. After injecting coarse particles and mixed with fine powders in the downer, the fluctuation of v_p in the radial direction becomes

Table 4 Operational conditions in the literature and present work

Ref.	Material	\bar{d}_p , mm	ρ_p , kg·m ⁻³	H , m	D_t , m	H/D_t	Number of data
[10]	FCC catalyst	0.067	1500	9.3	0.1	93	56
[13]	FCC catalyst	0.053	1348	5.8	0.14	41.4	40
[11]	FCC catalyst	0.067	1500	9.3	0.1	93	30
[14]	Glass bead	0.060	2658	8.6	0.15	57.3	50
this work	FCC catalyst	0.071	1500	0.6	0.03	32.8	32
	Glass bead	0.592	2658				112

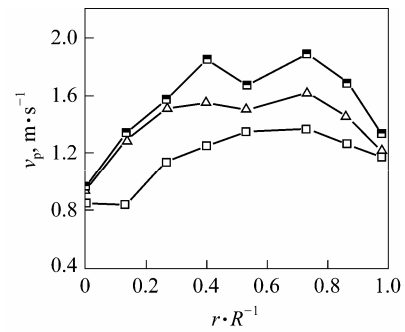
Note: Taking an equivalent diameter $D_e=4r_H$ to be the downer diameter D_t in this study.

**Figure 6** Radial distributions of binary mixture particle velocity at $u_g=1.97\text{m}\cdot\text{s}^{-1}$, $M^*=0.15$

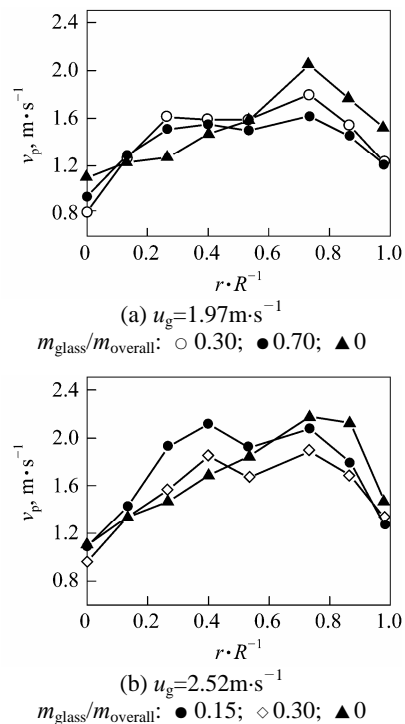
smaller due to the dispersing character and flow structure being improved.

At a constant M^* and when the gas velocity u_g is increased from $1.41, 1.97\text{m}\cdot\text{s}^{-1}$ to $2.52\text{m}\cdot\text{s}^{-1}$, the double peak distribution of v_p along the radial direction becomes more and more obvious either in $u_g=1.97\text{m}\cdot\text{s}^{-1}$ or in $u_g=2.52\text{m}\cdot\text{s}^{-1}$, which displays the gas velocity has a sufficient effect on the radial distribution of v_p as pointed out in Fig.7. Here the v_p is measured directly by using a fiber-optic probe and the PV-4A velocity instrument under $M^*=0.3$ and it only represents the local particle velocity (v_p) of this mixture.

When the composition ratio M^* is changed from 0.15, 0.30 to 0.70 as shown in Fig.8, the radial distribution of v_p still exhibits the shape of double peak distribution, *i.e.*, one peak occurs around $r\cdot R^{-1}=0.4$ and another at $r\cdot R^{-1}=0.733$. However, at the lower gas velocity $u_g=1.97\text{m}\cdot\text{s}^{-1}$ the peak around $r\cdot R^{-1}=0.4$ is not clear and the whole radial distribution of v_p for the binary mixture is more smooth in comparison with that of single parti-

**Figure 7** Radial profiles character of 70% FCC+30% glass bead 1 particle velocity ($Z=335\text{mm}$; $G_p=12.4\text{kg}\cdot\text{m}^{-2}\cdot\text{s}^{-1}$)
 $u_g, \text{m}\cdot\text{s}^{-1}$: □ 1.41; △ 1.97; ■ 2.52

cle FCC. The less M^* , the larger v_p and the more distinct of the double peaks, but the effect of M^* on the smoothness of the radial distribution of v_p is not observable. At the higher gas velocity $u_g=2.52\text{m}\cdot\text{s}^{-1}$ two peaks are also present at $r\cdot R^{-1}=0.4$ and $r\cdot R^{-1}=0.733$ in Fig.8.

**Figure 8** Effect of solids circulation ratio on radial profiles of mixture particle velocity (FCC catalyst and glass bead 1 mixture)

From the above experimental results by measuring the radial distribution of v_p for the binary mixture, it can be found that injecting coarse particles at the upper entrance into the downer benefits the smooth and uniform radial distribution of v_p for the binary mixtures. If injecting the coarse inert particles and fine coal simultaneously into the thermo-plasma downer reactor, both particles, around the center plasma jet region, will fall down the downer and the coarse inert particles can act as the coking carrier, which has been mentioned in the above section 2.3 when injected inert MC particles in the LPG thermo-plasma cracking. The smoothness of the radial distribution of v_p maybe avail to the reaction in the thermo-plasma coal cracking process since both of the fine coal and coarse inert particles may have respectively more similar resident time along the radial direction at the same axial distance of downer reactor.

The radial distribution of v_p for binary mixture were affected also distinctly by the injecting mode and the type of entrance distributor. More detailed results are referred to Zhu's thesis[15]. However, for industrial production requirements and throughput improvement, M^* below 15% may being a better selection for TPCPP, since the yield of acetylene production is in inverse proportion to M^* , which needs further experimental investigation.

4 CONCLUSIONS

According to experimental observation and investigation on both hot and cold mode experiment in downers, the following remarks can be given:

(1) The appropriated diameter of coarse MC particles can be used as an inert coking carrier and wall scourer to restrain or prevent the coking precursor material, produced from LPG or fine coal, from depositing on the downer walls and forming the coke. Therefore, a stable and continuous operation can be achieved in TPCPP to produce acetylene gas from coal fines.

(2) The gas and solids flow development in the downer and the radial distribution of the local particle velocity are related with many parameters, such as the axial position, gas velocity, solid cross-sectional flow rate and particle properties. At a certain axial position, gas velocity and solid cross-sectional flow rate, the radial distribution of the local particle velocity will being smoother when increasing the particle size and its density.

(3) For fine FCC particles with the aeration and agglomerating properties, which will cause greater gradient of particle velocity in the radial position. For coarse glass beads with unagglomerating properties, the less effect of wall friction will result in a smooth radial profile. The dimensionless local particle velocity v_p^* (ratio v_p/u_g) can be predicted by an empirical correlation based on the ratio r/R , H/D_t (the ratio of height to diameter of downer), $G_p/(u_g\rho_p)$ (the dimensionless mean section particle velocity assuming particles fully fill the whole section of downer).

(4) After injecting coarse particles and mixed with fine powders in downers, the fluctuation of local

particle velocity along the radial direction becomes smaller and two peaks in the radial distribution of local particle velocity occur due to the particle dispersion and flow structure being improved. The more uniform profile of local particle velocity of binary mixtures is beneficial to the thermo-plasma coal cracking reaction and coking prevention, since the coarse inert particles as the coking precursor carrier can take the coke away.

NOMENCLATURE

D_t	downer diameter, mm
\bar{d}_p	mean particle diameter, mm
G_s	solid cross-sectional flow rate, $\text{kg}\cdot\text{m}^{-2}\cdot\text{s}^{-1}$
H	downer length, mm
R	downer radius, mm
R_{ck}	coking rate per unit time, $\text{g}\cdot\text{s}^{-1}$
u_g	superficial gas velocity, $\text{m}\cdot\text{s}^{-1}$
v_p	local particle velocity, $\text{m}\cdot\text{s}^{-1}$
v_p^*	dimensionless local particle velocity, $\text{m}\cdot\text{s}^{-1}$
Z	axial distance in downer, mm
ρ_s	particle density, $\text{kg}\cdot\text{m}^{-3}$

REFERENCES

- Bond, R.L., Galbraith, I.F., Lander, W.R., "Production of acetylene from coal using a plasma jet", *Nature*, **200**, 1313—1314 (1963).
- Chakravarty, S.C., Dutta, D., Lahiri, A., "Reactions of coal under plasma conditions: direct production of acetylene from coal", *Fuel*, **55**, 43—46(1976).
- Baumann, H., Bitter, D., "Pyrolysis of coal in hydrogen and helium plasma", *Fuel*, **67**, 1120—1123(1988).
- Heinz, G.B., Baumann, H., Bitter, D., Kiein, J., Juntgan, H., "Pyrolysis of some gaseous and liquid hydrocarbons in hydrogen plasma", *Fuel*, **67**, 1012—1016(1988).
- Shen, B., Wu, Y., Gao, J., van Heek, K.H., "Study on the acetylene making by coal plasma pyrolysis", *Coal Conversion (China)*, **11**(4), 67—72(1994). (in Chinese)
- Tian, Y., "Study on the reactions of coal in arc plasma jet", Ph. D. Thesis, Taiyuan University of Technology, China (2001). (in Chinese)
- Zhu, Y., Zhang J.Y., Xie, K., "Research progress on the acetylene production from coal cracking in thermal plasma downer", *J. Chem. Ind. Eng.*, **25**(1), 30—36(2004). (in Chinese)
- Bittner, D., Baumann, H., Klein, J., "Reaction between coal properties and acetylene yield in plasma pyrolysis", *Fuel*, **64**, 1370—1374(1985).
- Lü, Y., Tian, Y., Wang, D., Xie, K., Zhu, S., "Influence of granularity on coal pyrolysis in Ar/H₂ plasma", *J. Fuel Chem. Tech.*, **20**(3), 229—233(2002). (in Chinese)
- Zhang, H., Zhu, J.X., Maurice, A., "Flow development in a gas-solid downer fluidized bed", *Can. J. Chem. Eng.*, **77**, 194—198(1999).
- Zhang, H., Zhu, J.X., "Hydrodynamics in downflow fluidized beds (2) Particle velocity and solid flux profiles", *Chem. Eng. Sci.*, **55**, 4367—4377(2000).
- Zhu, Y., Zhang, J.Y., Xie, K., "Radial distribution characteristics of local particle velocity for binary particle mixture in downers", *J. Chem. Ind. Eng. (China)*, **55**(11), 1777—1786(2004). (in Chinese)
- Yang, G.Q., Wei, F., Wang, Z., Jin, Y., "The application of LDV technique to measure two-phase flow in a gas-solid concurrent upflow and downflow CFB", *Experiments and Measurements in Fluid Mechanics*, **11**, 15—17(1997). (in Chinese)
- Lehner, P., Wirth, K.E., "Characterization of the flow pattern in a downer reactor", *Chem. Eng. Sci.*, **54**, 5471—5483(1999).
- Zhu, Y., "Experimental study on particle flow characteristics in downer", Master Thesis, Fuzhou University, China (2004). (in Chinese)